Democratic and Popular Republic of Algeria
Ministry of Higher Education and Scientific Research
Larbi Tebessi University-Tebessa-

Faculty of science and technology

Dissertation Submitted in Partial Fulfillment of the Requirements For
The Degree of **Master** of **Science** 2sd cycle
In : Mechanical Engineering
Speciality : Energitics

By : Djabir Tamrabet

Subject

Design, Performance Analysis and Realization of an Axial Flow Fan

Publicly defended, On 24/06/2021, in front of:

Mr.	Abdelkarim Bouafane	MCB	Tebessa	President
Mr.	Ramzy Medouki	MCA	Tebessa	Advisor
Ms.	Latifa Zaidi	MAA	Tebessa	Examiner

Dedication

To my dad, brothers and sisters as well as my best friends for their continuous motivation to strive for excellence. To all my teachers in the mechanichal engineering department I could not have done this without, and last but not least to all my colleagues.

acknowledgements

I offer my deepest gratitude to my academic and research advisor Dr. Medouki Ramzi, for giving me this wonderful opportunity to work on this project. His continuous encouragement, guidance at every juncture of the research and unceasing faith in me has been extremely helpful. He was always available to answer my (technical as well as career related) questions whenever I needed a sense of right perspective, giving his time and knowledge liberally.

abstract

Axial flow fan is one of the most important turbomachinery used in our daily life. It spreads in various forms and types, and it is identified according to the needs and characteristics of the application field. To this end, the main purpose of this thesis is designing and printing a three-dimensional(3D) model of an axial flow fan with predefined characteristics, which is addressed to be used inside a wind tunnel for scientific experiments that deal with measuring the aerodynamics properties of airfoils used in turbomachinery . From a modeling point of view, the CFturbo software is used for the sake of coming up with the needed model, to emphasize, the isolated airfoil method as well as the radial equilibrium approach are employed along the process of the desired model. Concerning the analysis phase, the numerical analysis is carried out by means of Gambit software and then the grid information are exported to Ansys Fluent including the different boundary-initial conditions and the turbulence model K-epislon taking into account the convergence conditions. Having said that, the desired target is not achieved due to the unavailability of solution. Ultimately, the studied model was printed using a 3D printer Creality Ender 3 (35X30X20). Then, the designed model is used as a source of air within the wind tunnel.

الملخص

تعتبر المراوح المحورية من أهم الالات التوربينية المستعملة في حياتنا اليومية واكثرها انتشار وفق أشكال وأنواع مختلفة و كذلك خصائص متباينة و ذلك حسب الحاجة ومجال الاستعمال.

على هذا الضوء كان الهدف من هذه المذكرة هو تصميم وطباعة نموذج ثلاثي الابعاد لمروحة ذات خصائص محددة موجهة للاستعمال داخل نفق هوائي من اجل اجراء التجارب العلمية لقياس الخصائص الايروديناميكية لمقاطع الاجنحة المستعلمة في الآلات التوربينية.

في مرحلة التصميم تم استعمال البرنامج المعلوماتي CFturbo حيث تم اختيار الوحدة الخاصة بتصميم المراوح المحورية واعتماد طريقة الجنيح المعزول ومقاربة التوزان القطري من اجل تصميم النموذج المطلوب.

فيما يخص التحليل باستعمال وسيلة الحساب العددي تم تشكيل شبكة الحسابات باستعمال برنامج Gambit و من ثم ادراج احداثيات الشبكة في البرنامج Ansys-Fluent مع مختلف الشروط الحدية و الابتدائية و نموذج العصف K-ε و شروط التقارب، الا انه لم يتم الحصول على حل يتم من خلاله تحليل النموذج المدروس.

في المرحلة الأخيرة الخاصة بالانشاء، تم طباعة النموذج المدروس وذلك باستعمال الطابعة الثلاثية Creality Ender 3

ذات الأبعاد (35X30X20) و من ثم استخدام النموذج المصمم في النفق الهوائي كمصدر لتوليد جريان الهواء.

Nomenclature

1	Inlet
2	Outlet
s	Pitch length
r_m	mean radius
r_h	Hub radius
r_t	Tip radius
z_b	Number of blades
F_L	Lift force
F_D	Drag force
ρ	Density
c_l	Lift coefficient
c_d	Drag coefficient
W_m	Relative mean velocity
b	Span length
Q	Volumetric flow rate
$\Delta_p t$	Totale pressure difference
N, n	Rotational speed
D	Diameter
n_q,σ	Specific speed
δ	Diameter number
ν	Hub-tip ratio
D_h	Hub diameter
D_t	Tip diameter
φ	Flow coefficient

C_u	Meridional velocity
u	Tangential velocity
Ψ	Work coefficient
Υ	Specific work
α_i	Absolute flow angle
β_i	Relative flow angle
C_{ax}	Axial velocity component
c	Absolute velocity
W_u	Tangential component of relative velocity
C_u	Tangential component of absolute velocity
ξ	Stagger angle
α	Angle of attack
ε	Glid ratio

Contents

Dedication ii

acknowledgements iii

abstract iv

Nomenclature vi

List of Figures ix

List of Tables x

Introduction 2

1 Generality on Axial Flow Fans 3

1.1 General Information on Axial Flow Fans 3

1.2 Classification of Axial Flow Fans 4

1.2.1 Propeller Fans 4

1.2.2 Tube-Axial Fans 6

1.2.3 Vane-Axial Fans 7

1.2.4 Two-Stage Axial Fans 8

1.3 Performance of Axial Flow Fans 9

2 Design Theory of the Axial Flow Fan 11

2.1 Introduction 11

2.1.1 Axial Flow Fan blade design methods 11

2.2 Isolated Airfoil Approach 12

2.3 Preliminary Design Procedure 14

2.3.1 Cordier Diagram 14

2.3.2 Hub-Tip Ratio and Specific speed Relationship 16

2.3.3 Head and flow coefficients 17
2.3.4 Free Vortex Design Method and Velocity Diagrams 18

3 Software Implementation 21
3.1 Introduction 21
3.2 CFturbo Software Overview 21
3.3 Axial Flow Fan Design Steps By CFturbo 22
3.3.1 Specifying The Design Point Values 22
3.3.2 Impeller Main Dimensions 23
3.4 Impeller Meridional Contour 28
3.4.1 Primary Flow Path 28
3.4.2 Hub/Shroud solids 29
3.5 Blade's Geometry Design 31
3.5.1 Blade properties 31
3.5.2 blade profile 36
3.5.3 Blade sweeping 37

4 CFD Analysis of the Axial Flow Fan 39
4.1 Introduction 39
4.2 Geometry 40
4.3 Computation Mesh 40
4.4 Boundary Conditions 41
4.5 Turbulence Model and Solver Options 42

General Conclusion 43

Bibliography 44

List of Figures

1.1 Axial flow fan's Sketch . . . 3
1.2 Propeller fan with direct drive . . . 5
1.3 Propeller fan with belt drive . . . 5
1.4 Tube-axial fan with direct drive . . . 6
1.5 Tube-axial fan with belt drive . . . 6
1.6 Vane-axial fan with direct drive . . . 7
1.7 Vane-axial fan with belt drive . . . 7
1.8 Two-stage axial fan . . . 8
1.9 Typical features of axial flow fans with direct drive . . . 9
1.10 Performance curves of an axial flow fan . . . 10

2.1 The pitch distance between two adjacent fan blades . . . 12
2.2 Forces acting on isolated airfoil . . . 13
2.3 Characteristics curves for NACA airfoil 6512 . . . 14
2.4 The Cordier diagram . . . 16
2.5 The optimum Hub-Tip ratio in terms of specific speed . . . 17
2.6 Chart of ψ versus ϕ for various fans and pumps . . . 18
2.7 Axial flow fan velocity triangles . . . 19
2.8 Stagger angle versus angle of attack . . . 20

3.1 CFturbo main window . . . 22
3.2 Design point values and machine type . . . 23
3.3 Impeller main dimensions (General setup) . . . 24
3.4 Impeller main dimensions (Empirical parameters) . . . 24
3.5 Approximation function (Hub-tip ratio) . . . 25
3.6 Values of hub and tip diameters . . . 25
3.7 Results of mid-span calculation . . . 26
3.8 Velocity triangles . . . 27

3.9 Primary flow path 28
3.10 Hub solid 29
3.11 Meridional contour global information 30
3.12 Hub 3D model 30
3.13 Number of blades in accordance to specific speed 31
3.14 Number of blades in accordance to specific speed 32
3.15 Numerical values of velocity components and flow angles at hub and shroud 33
3.16 Number of blades in accordance to specific speed 34
3.17 Properties of the blade profile 35
3.18 Blade stagger angle and chord length at different span 35
3.19 2D profiles and thickness distribution at different span 36
3.20 3D blade profiles 37
3.21 3D axial flow fan model 38

4.1 The Axial fan single 3D blade shape inside the flow domain 40
4.2 Computational mesh of the solution domain 41
4.3 Fan Boundary Conditions (1) 42
4.4 Fan Boundary Conditions (2) 42

List of Tables

1.1 Difference between fans, blowers and compressors 4

3.1 Design point values and machines type 22
3.2 The used formulas for calculating some variables 26
3.3 Nomenclture 33

Introduction

When airflow is crucially required but does not occur naturally, fans are then utilized to generate it . As a result, fans are largely employed in both commercial and industrial applications. From shop ventilation to material handling to boiler applications and HVAC systems, they are critical for process support and have significant implications for plants performance, production and also efficiency. This diverse and widespread usage of fans, imply various models with distinct physical construction, and thus distinctive physical proprieties of each sort of fan since each form is designed for a particular purpose. For instance, in specific mining industry operations, providing adequate fresh air volumes to the operational area is imperative so as to maintain a safe and productive work environment. Hence, the primary design challenge is procuring the requisite pressure difference to convey the appropriate amount of air[1]. Furthermore, the major function of a cooling fan that is used in a cooling system is blowing hot air away as well as limiting the heating rate, by maintaining the temperature of a structure or a device from surpassing limitations imposed by demands of safety and efficiency, thereby fan airflow capacity becomes more critical as the cooling process is directly related to the flow rate. In that situation, physical features of the fan should be set up considering the air velocity and large fan diameter, which assist in producing considerable volumes of air. Interestingly, fans placed inside roadway tunnels as ventilation systems are purposefully constructed to fit in with the airfoil profile that enables these fans to blow air bi-directionally in response to the changing needs once the rotational direction is reversed[2].

The subject of this thesis is the design, performance analysis and realization of a tube, unvaned axial flow fan used for wind tunnel. From a designing point of view, the model of the fan is generated based on the commonly employed empirical methodologies in the literature, using a sophisticated and compatible turbomachinery design software. In the numerical analysis phase, the model is analyzed through a Commercial Fluid Dynamics (CFD) software which includes determining the appropriate mesh type, boundary conditions, and solution approach as well as turbulence model. Ultimately,

in the realization stage, the necessary adjustments to the model are made via CAD software (due to assembly concerns) and then is printed using a three-dimensional printer.

Chapter 1

Generality on Axial Flow Fans

1.1 General Information on Axial Flow Fans

In its most basic geometrical construction an axial flow fan stage consists of a rotor made up of two to fifty blades fitted to the hub, the flow is then established through the rotor once the fan shaft starts rotating around its axis by means of a particular driving motor type, which is often an electric motor with three main potential arrangements: belt drive, direct drive, and gear drive [3]. Additionally, in axial fans, the working fluid is sucked and discharged axially, namely in the same direction as the axis of the rotating shaft. The working[**?**] fluid is typically air that is operated at low speed (M 0.3), and consequently the change in air density considered insignificant and the effect of Mach number is negligible.

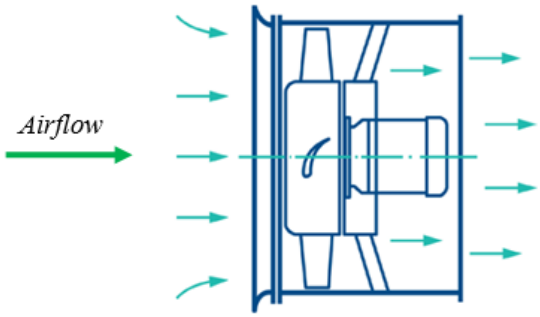

Figure 1.1: Axial flow fan's Sketch

According to the American Society of Mechanical Engineering (ASME), axial fans have a maximum pressure ratio on the order of 1.11, they differ from other devices such as blowers and compressors in the manner they move air as well as the pressure rise

they can possibly attain. The specific characteristics of an axial fan are heavily affected

Table 1.1: Difference between fans, blowers and compressors

Equipement	Pressure ratio	Pressure rise (bar)
Fans	Up to 1.11	0.11
Blowers	1.11 to 1.20	0.11 - 0.20
Compressors	More than 1.20	0.20 onwards

by the aerodynamic design and number of impeller blades, and also the angle they present to the oncoming airstream. Some axial impeller designs allow the blade angle to be controlled either while stationary or in motion. Ideally, the flow passes axially over the impeller with no tangential velocity component and the requisite pressure rise results from an increase in the impeller tangential velocity and subsequent aerodynamic diffusion.

Axial fans are widely employed in applications requiring high flow rates and low pressure. They are employed for ventilation and air conditioning of subterranean transit networks, mines, and structures, in addition to a wide range of usage in a variety of industries from power plants to cooling towers and steel factories and many other industrial activities. Each application entails a particular type of fan to handle the system necessities, hence certain fans are more suitable than others in terms of capacity and in this regard, axial fans are grouped into four varieties.

1.2 Classification of Axial Flow Fans

1.2.1 Propeller Fans

Propeller fans, sometimes known as panel fans, are the most basic, least cost, and extensively used type. These fans have a modest pressure rise but generate high airflow volumes. They typically consist of a flat frame or housing to be mounted on a wall or on a partition, and they are used as exhaust fans to remove hot or contaminated air from facilities. Additionally, there are two different types of drive arrangements for propeller fans: direct drive and belt drive arrangement.

In the direct drive arrangement, the electric motor is directly attached to the rotor of the fan. In comparison to the belt drive configuration, production cost is reduced as the belt and pulleys are not being used and in terms of efficiency, the direct drive method is more efficient since no additional power is consumed via belt and pulleys.

Figure 1.2: Propeller fan with direct drive

Figure 1.3: Propeller fan with belt drive

In the belt drive arrangement, the rotating motion of the electric motor is conveyed employing a belt and pulleys. Belt drive gives versatility in its performance as any rotating speeds for the fan wheel can be acquired by selecting the right pulley ratio and also it is preferred in big sizes because it keeps the fan wheel speed low or moderate while maintaining the motor speed high, resulting in cheaper costs since high-speed motors are less expensive than low-speed motors of the same horsepower[4].

1.2.2 Tube-Axial Fans

Tube-axial fans are similar to propeller fans. Nevertheless, they possess different physical characteristics. Their hub-tip ratio ranges from 0.3 to 0.5 whereas propeller fans' hub-tip ratio is less than 0.3. Moreover, tube axial fans can generate higher pressure rise and operate more efficiently.

This type of fan is characterized by an external cylindrical housing in which the drive motor is positioned on either the inlet or outlet side, whereas in the belt drive case, the motor is situated outside[4].

Figure 1.4: Tube-axial fan with direct drive

Figure 1.5: Tube-axial fan with belt drive

1.2.3 Vane-Axial Fans

Vane-axial fans are identical to tube-axial fans, but they are equipped with guide vanes to enhance efficiency by guiding and straightening the flow. The guide vanes are housed inside a cylindrical housing that has a length of one diameter long, and they can be employed either before or/and after the rotor. As upstream guide vanes they adjust the inlet angle of incoming flow, and as downstream guide vanes they neutralize the air spin and convert part of the excess velocity pressure into more useful static pressure.

Compared to the earlier fan types, vane-axial fans can deliver higher flow rates and generate higher static pressure rise at a larger hub-tip ratio ranging from 0.5 to 0.8. Similarly, they can also be operated with or without belt and pulleys by employing an electric motor[4].

Figure 1.6: Vane-axial fan with direct drive

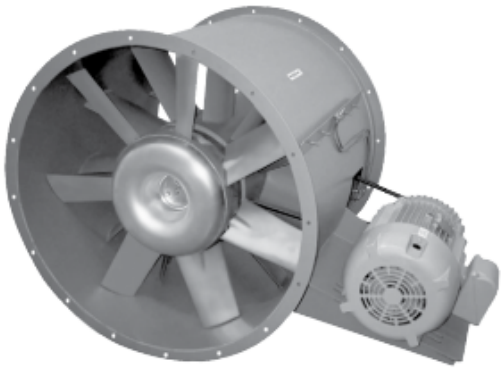

Figure 1.7: Vane-axial fan with belt drive

1.2.4 Two-Stage Axial Fans

Two-stage axial flow fans have the configuration of two fans in series so that the pressures will add up. This is an easy solution when higher static pressures are needed, but excessive tip speeds and noise levels are not tolerated.

The tow fan wheels may rotate in the same direction, with guide vanes between them. Or they may be counter-rotating, without any guide vanes. By either method, the static pressure will be doubled.

In the first configuration, each of the two fans is operated by two separate motors or a single double-shaft extension motor placed between the two stages. The stationary guide vanes are also between the two fan wheels. They pick up the helical airflow produced by rotating blades of the first stage and reverse the rotational component to the opposite direction, whereby the air velocity first decelerates and then accelerates again. Namely, they act as outlet vanes for the first stage and as inlet vanes for the second stage.

In contrast, in the second configuration, the two fan wheels run in opposite directions and are driven by two separate motors. The air spin produced by the first stage is more or less neutralized by the deflection produced by the second stage. As a result, no guide vanes are needed, which reduces the manufacturing cost somewhat. Another advantage of this configuration is that if one of the two motors fails, the unit can still deliver some air while only one stage is operating[4].

Figure 1.8: Two-stage axial fan

Typical features of axial flow fans with direct-drive arrangement are given in the following table:

	Propeller Fan	*Tube-Axial fan*	*Vane-Axial fan*	*Two-stage axial-flow fan*
Casing	Mounting ring or panel	Short cylindrical housing	Cylindrical housing	Long cylindrical housing
Motor Support	Inlet side of panel preferred	Inside housing,outlet side preffered	Inside housing, outlet side preffered	Inside housing, between the two stages
Guide Vanes	None	None	Past fan wheel preferred	Between the two stages or none
Hub-Tip ratio	< 0.3	0.3 - 0.5	0.45 - 0.8	0.5 - 0.8

Figure 1.9: Typical features of axial flow fans with direct drive

1.3 Performance of Axial Flow Fans

Specific tests are used to assess the performance of axial flow fans. These tests are accomplished according to a set of guidelines, carried out in laboratory tests under specific conditions. These fan guidelines were developed with the help of the Air Movement and Control Association, Inc. (AMCA) and the American Society of Heating, Refrigeration, and Air Conditioning Engineers, Inc. (ASHRAE). They develop standardized techniques for calculating fans' flow rate, pressure increase, power consumption, and efficiency, and thereby these parameters are used to form a fan's performance curves. An example of axial flow fan performance curves is depicted in figure 1.9[1].

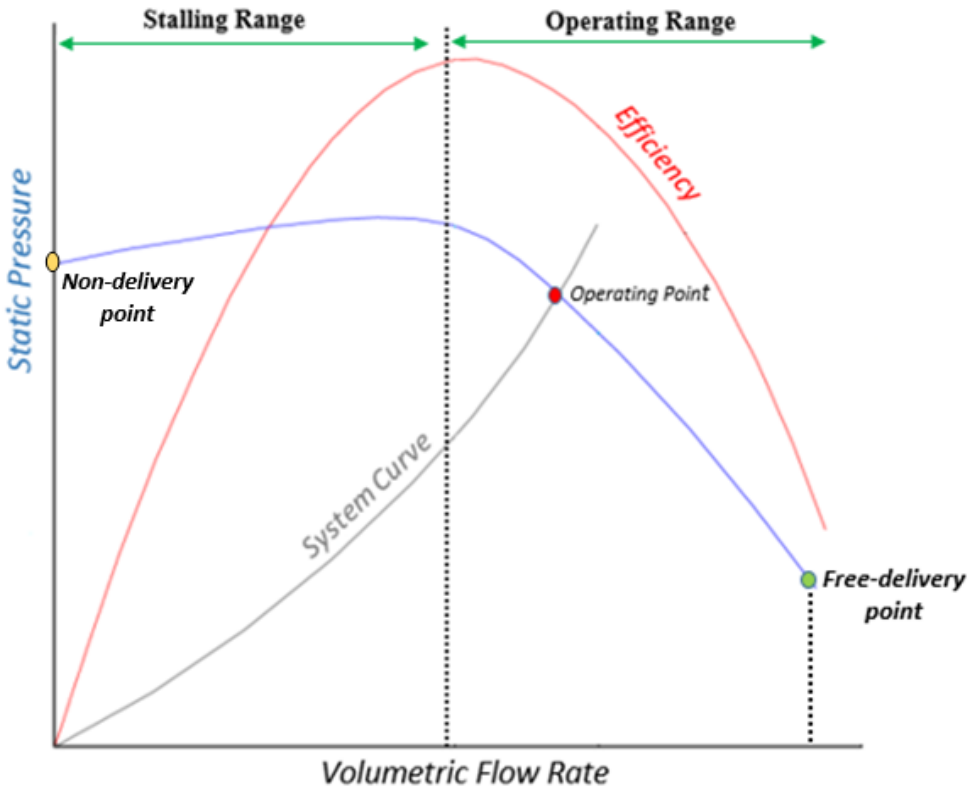

Figure 1.10: Performance curves of an axial flow fan

In figure 1.9, it is shown the shape of a typical static pressure versus volumetric flow rate curve of an axial flow fan. Starting at the free-delivery point (i.e., when the volumetric flow rate reaches its maximum while the static pressure approaches zero), the static pressure rises to a peak value from this point to the free-delivery point, this is the fan's good operating range within it, is located the operating point that represents the intersection of the fan characteristic curve with the system curve.

In this operating range, when the flow rate decreases owing to increased flow resistance, the axial air velocity drops as well. As a result, the angle of attack and lift coefficient both rise, resulting in an increase in static pressure as the flow rate falls.

Consequently, the operating point on the pressure curve shifts to the left, while static pressure rises to the stalling range. After the stalling range, static pressure begins to drop and then the fan can no longer operate effectively.

Chapter 2

Design Theory of the Axial Flow Fan

2.1 Introduction

The axial flow fan design is still dependent on many empirical and semi-empirical criteria stated by fan designers, resulting in a variety of approaches to designing fan components and, more specifically, fan impellers. At the outset of the fan design process, the design procedure consists in setting up the design point data as inputs. On that basis, the subsequent parameters and dimensions are determined. These input data are known as the design parameters, which mainly constitute the design specifications, mainly the volumetric flow rate, total pressure difference, rotational velocity of the drive motor, and fluid properties. The methodology, approaches, and empirical graphs utilized in the axial flow fan design, as well as the parameters employed in the design processes, are discussed and explained in this chapter.

2.1.1 Axial Flow Fan blade design methods

The fan blades' interaction has a considerable impact on the fan design since the lift and drag coefficients derived from a blade on the fan impeller, are dependently differed based on the distance between the neighboring blades, which is known as the pitch distance or spacing. This latter represents the distance in the direction of rotation between corresponding points on adjacent blades and can be seen in figure 2.1.

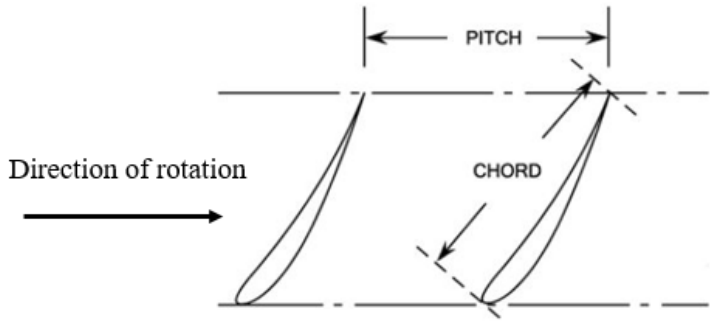

Figure 2.1: The pitch distance between two adjacent fan blades

The chord c and the pitch s of the blades are related, and this relationship is known as blade solidity. It is used to indicate whether or not the blades interact with one another. It can be expressed as:

$$sol = {}^{c}/_{s} \tag{2.1}$$

where $S = \frac{2\pi r_n}{Z_b}$ Where r_m is the mean radius of the fan, and z_b is the number of blades. In case of an axial flow impeller the mean radius is defined in terms of tip radius, r_t and hub radius, r_h of the fan as follows:

$$r_m = \sqrt{\frac{\left(r_t^2 + r_h^2\right)}{2}} \tag{2.2}$$

There are two main approaches to designing an axial flow fan blade which can be summed up as: the isolated airfoil approach and the cascade approach. The decision of which approach is employed in the blade design is based on the blade solidity calculation. Whereas the isolated airfoil approach is valid for low solidities less than one, cascade approach is valid for high solidities greater than one[5].

2.2 Isolated Airfoil Approach

In the isolated airfoil method, a control volume is created around a single airfoil. Once a flow field is established to this control volume, the airfoil will be impacted by several forces operating in different directions. More precisely, as the flow field moves through the airfoil it normally it produces positive pressure on the lower surface (pressure side) of the airfoil and negative pressure on the upper surface (suction side), the combination of these positive and negative pressures results in a force F, as shown in figure 2.2. This force F can be resolved into two components, a lift force F_L and a drag force F_d .

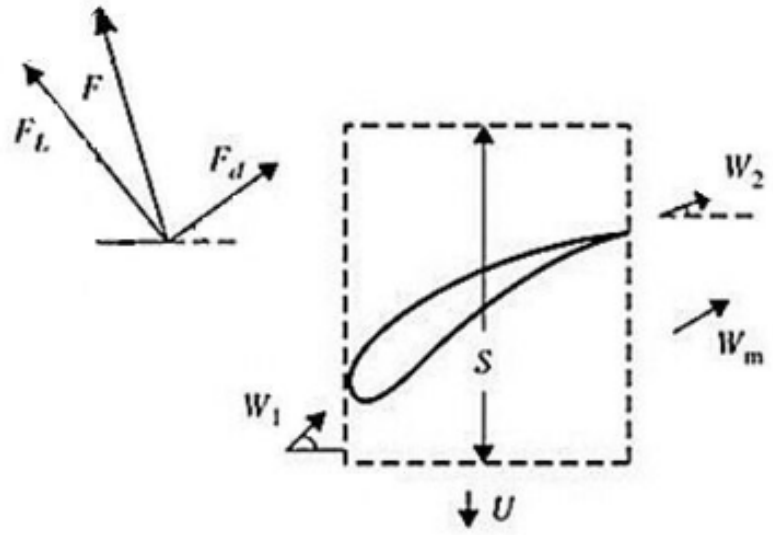

Figure 2.2: Forces acting on isolated airfoil

The drag force F_d is parallel to the direction of the relative mean velocity w_d, while the lift force F_L is normal to the drag force. In the case of an axial flow fan blade the lift force considered the useful component since it deflects the air stream and produces the static pressure of the fan, whereas the drag force is the resistance to the forward motion of the blade, it's the undesirable, power-consuming component[4].

Therefore we should use an appropriate airfoil shape that have not only a high lift coefficient c_L but also an appropriate lift-drag ratio $\frac{c_L}{c_d}$.

As the angle of attack changes, lift, drag, and lift-drag ratio all change considerably, as it is shown in figure 2.3. The lift and the drag forces can be expressed in terms of the lift and the drag coefficients c_L and c_D respectively, as follows

$$F_L = c_L bc\left(\frac{\rho w_m^2}{2}\right) \tag{2.3}$$

$$F_D = c_D bc\left(\frac{\rho w_m^2}{2}\right) \tag{2.4}$$

Where b is the span length of the fan blade and w_m is the relative mean flow velocity.

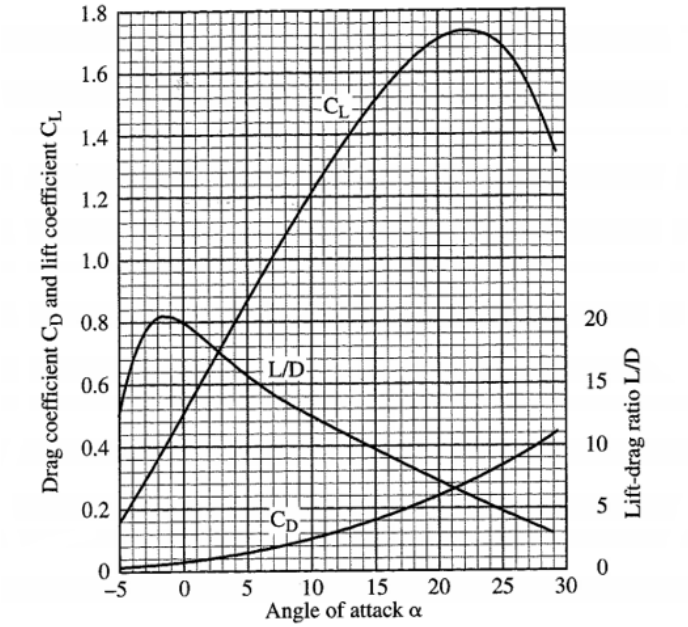

Figure 2.3: Characteristics curves for NACA airfoil 6512

2.3 Preliminary Design Procedure

At the beginning of the design process, various input parameters are essential to define the starting point, which are the volumetric flow rate Q, the total pressure difference Δp_t and last but not least, the rotational speed n of the motor drive. This latter is directly related to the rotational velocity of the fan impeller, and as the machine is set to operate in an incompressible range where Mach number is less than 0.3, and as the attained tangential velocity at the tip of the blade is the highest speed for the axial flow fan, the rotational speed must be selected reasonably otherwise the fan may found working in inappropriate conditions.

2.3.1 Cordier Diagram

In order to design an efficient turbomachine, the Cordier diagram is regarded as an unavoidable tool to consult. The Cordier diagram is an empirical diagram based on measurements, that depicts the relationship between the design parameters and the different types of turbomachines, using two dimensionless numbers, the specific speed (speed number) and the diameter number. Which can be expressed sequentially as follows:

$$\sigma = \frac{E}{H} \tag{2.5}$$

knowing that : $E = N\sqrt{Q}$ and H= $\left(\Delta\rho/\rho\right)^{1/4}$

Where, N and D are respectively the rotational speed and the diameter of the required machine. Furthermore, though this diagram does not illustrate the specifics of the blade form for turbomachines design, it is indisputably valuable in obtaining fundamental selections regarding the type of the machine being used for a certain operating point. Usually, once given a specific motor drive and hence a rotational speed, as well as a specified operating point, the Cordier diagram can be used to determine the kind of machine (axial, diagonal, or radial) and the diameter of the impeller that would best fulfill this operating point. If, on the other hand, a specific operating point must be achieved with an impeller of a specific diameter, the Cordier diagram can easily be used to determine the rotation speed that will achieve this point with the greatest efficiency. As a result, whenever layout considerations in turbomachines are done, the Cordier diagram is often employed[6]. The different classifications of impeller types According to the speed number and diameter number are shown on the Cordier diagram in figure 2.4

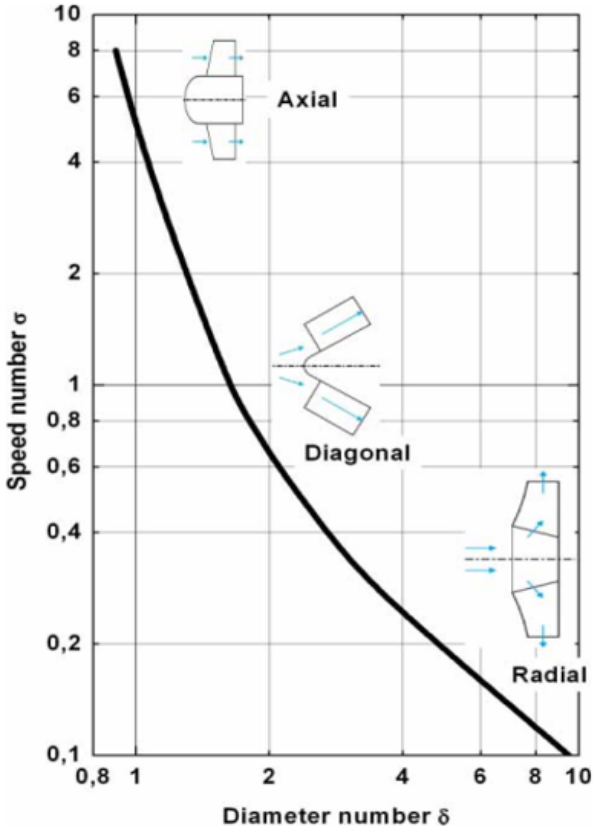

Figure 2.4: The Cordier diagram

2.3.2 Hub-Tip Ratio and Specific speed Relationship

The hubtip ratio represents a characteristic geometric dimension of the axial fan blade and it usually defined as follows:

$$v = \frac{D_h}{D_t} \tag{2.6}$$

where D_h is the hub diameter and D_h is the diameter tip As stated in the previous chapter, the axial flow fans may be classified based on their hub-tip ratio, knowing that tube-axial fans have a hub-tip ratio ranging from 0.3 to 0.5, thus the determination of the hub-tip ratio value assists recognizing whether a particular fan design is within the design limit or not. For this objective, the specific speed and the design aspect are significant elements that determine the best possible choice of hub-tip ratio[7].

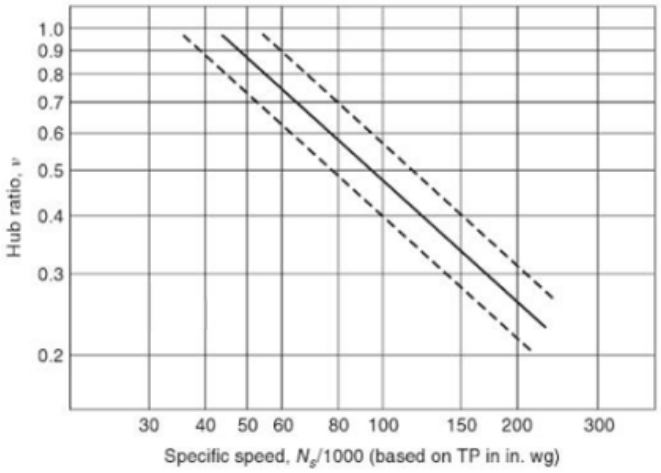

Figure 2.5: The optimum Hub-Tip ratio in terms of specific speed

2.3.3 Head and flow coefficients

To characterize operating behavior and design type in turbomachinery engineering, numerous characteristic coefficients are utilized. Affinity laws are used to determine these coefficients, which are calculated from physical quantities. From these dimensionless parameters we distinguish two often used values, the flow coefficient and the work coefficient[8]. The flow coefficient, also known as the volume coefficient, is used to characterize the volume flow rate and is defined as follows:

$$\varphi = \frac{c_m}{u} \tag{2.7}$$

Where, c_m is the meridional velocity and u is the local blade rotational speed. The work coefficient, occasionally named as the energy transfer coefficient, and the head coefficient, is used to describe the machine's head.

$$\psi = \frac{\Delta p}{\frac{1}{2}\rho u^2} \tag{2.8}$$

Another formula for the work coefficient is given as:

$$\psi = \frac{Y}{\frac{1}{2}u^2} \tag{2.9}$$

Where Y is the specific work, it is written as: $Y = \frac{\Delta\rho}{\rho}$. The chart of work coefficient versus flow coefficient ϕ for various fans and pumps is shown in figure 2.6.

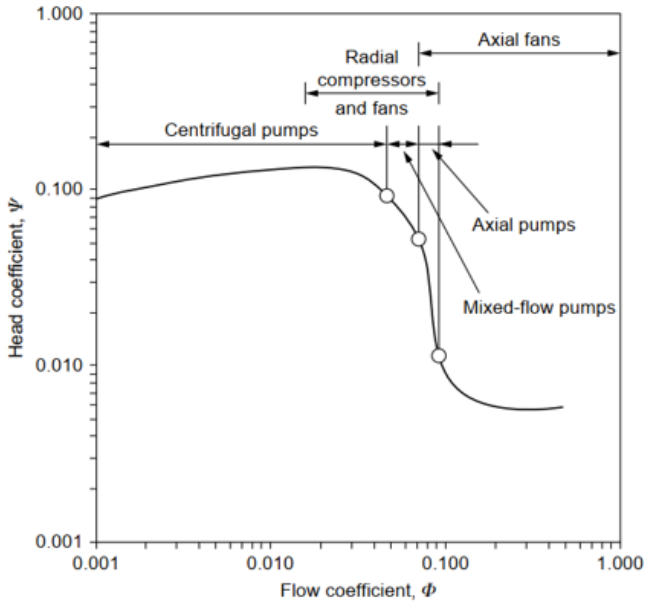

Figure 2.6: Chart of ψ versus ϕ for various fans and pumps

2.3.4 Free Vortex Design Method and Velocity Diagrams

In the airfoil approach, the fluid flow and blades are studied in a two-dimensional plane. In the radial direction, it is assumed that the flow has no radial velocity (i.e., the fluid velocity has no third component). Accordingly, the fluid flow as well as the blade profile are illustrated and analyzed on a two-dimensional plane.

Furthermore, the most widely used mode for designing axial flow fan blades, free vortex law is adopted in order to make a realistic blade design, by taking into account the radial variation in certain parameters, specifically the blade speed and the velocity flow tangential component. In this approach the product $c_u r$ is held a constant across the exit of each blade at different radial height, and the flow axial velocity component is assumed equal along the radius of the blade. Consequently from the flow axial velocity and the blade speeds the velocity triangles can be completed at various radial sections[9].

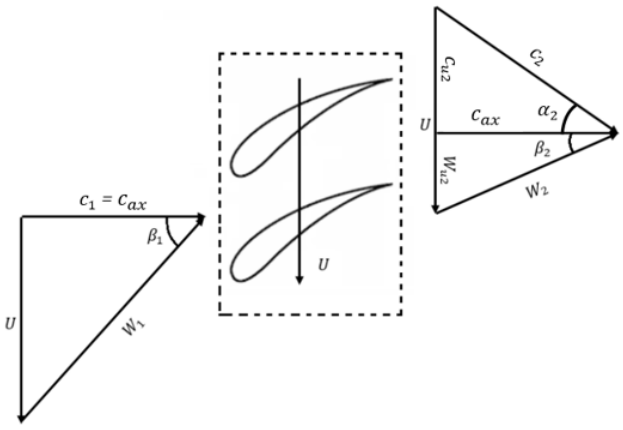

Figure 2.7: Axial flow fan velocity triangles

The flow angles α and β, depicted on the velocity diagram in figure 2.7, indicate the absolute flow angle and the relative flow angle, respectively. While the relative flow angle has two different values, one at the inlet and one at the outlet, the absolute flow angle has only one value (i.e. at the outlet) since it is null at the inlet. Interestingly, it can be noticed that the flow axial velocity component is constant throughout. The various flow angles can be determined using the following formulas:

$$\beta_1 = \tan^{-1}\left(\frac{U}{c_1}\right) \tag{2.10}$$

$$\beta_2 = \tan^{-1}\left(\frac{w_{u2}}{c_{ax}}\right) \tag{2.11}$$

$$\alpha_2 = \tan^{-1}\left(\frac{c_{u2}}{c_{ax}}\right) \tag{2.12}$$

Where, β_1 is the inlet relative flow angle, β_2 is the outlet relative flow angle and α_2 is the outlet absolute flow angle. U: is the tangential velocity, c_1 : is the absolute inlet flow velocity. They can be respectively given as:

$$U = wr \tag{2.13}$$

$$c_1 = \frac{Q}{\frac{\pi\left(D_t^2 - D_h^2\right)}{4}} \tag{2.14}$$

The relative inlet flow velocity w_1 and the relative outlet flow velocity w_2 are determined as:

$$w_1 = \sqrt{c_1^2 + U^2} \tag{2.15}$$

$$w_2 = \sqrt{c_{ax}^2 + w_{u2}^2} \tag{2.16}$$

Where, w_{u2} is the tangential component of relative outlet flow velocity. The stagger angle ξ of an airfoil in an axial flow fan configuration is defined as the angle between the axial direction and the chorde line, and it depends on both angle of attack as well as the angle of relative flow β.

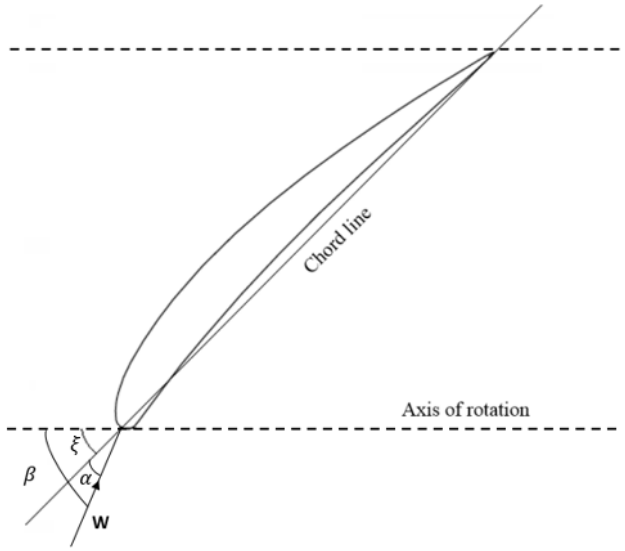

Figure 2.8: Stagger angle versus angle of attack

The stagger angle can be calculated as

$$\xi = \beta - \alpha \tag{2.17}$$

Chapter 3

Software Implementation

3.1 Introduction

Based on the key points for designing an axial flow fan impeller that are outlined in the previous chapter, it can be observed that the designing process is quite delicate since it incorporates varied designing approaches besides sustained turbomachinery and aerodynamics calculations. On this account, there is a demand for using such satisfactory turbomachinery designing software.

3.2 CFturbo Software Overview

Fturbo is a modern, powerful software for interactive design of turbomachinery (pumps, ventilators, compressors and turbines). It enables the designer to either start from the outset or redesign existing models. The main advantage of the software is the combination of fundamental conceptual design equations, proven empirical correlations and varied geometrical capabilities. Moreover, it includes several interfaces to established CAD and CFD packages for further processing of the designed geometry. Figure 1.3, shows the Cfturbo software's main window, from which the desired turbomachinery type can be selected.

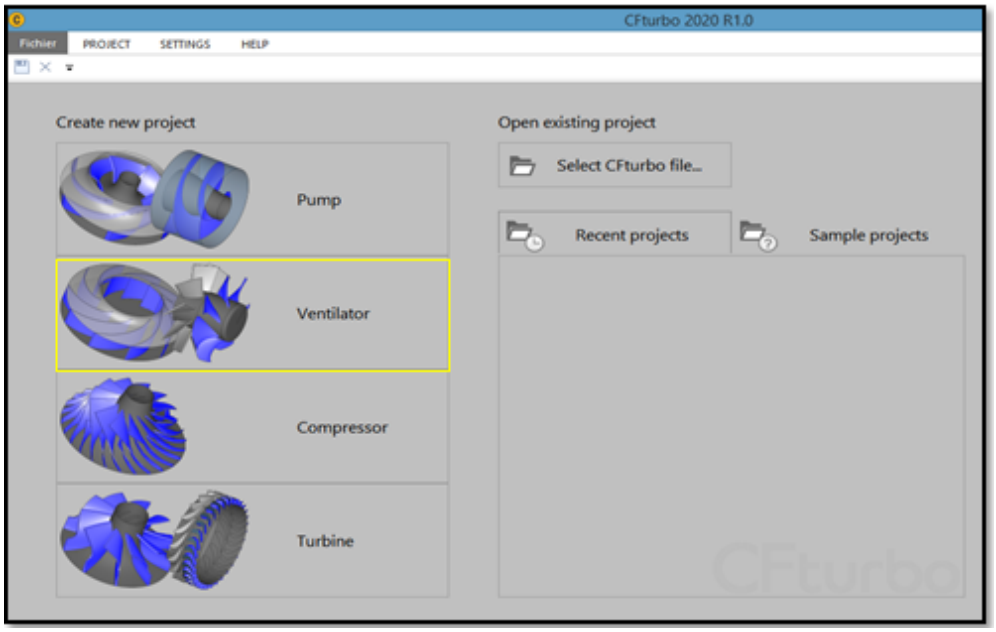

Figure 3.1: CFturbo main window

3.3 Axial Flow Fan Design Steps By CFturbo

3.3.1 Specifying The Design Point Values

The starting point is the definition of the design point comprising of volumetric flow rate, total pressure rise and rotational speed as well as fluid properties. The design point is defined as shown in the following table:

Table 3.1: Design point values and machines type

Flow Rate Q $\left[{m^3}/{s}\right]$	0.064
Totale Pressure difference Δp_t [Pa]	12
rotational speed n [rpm]	1300

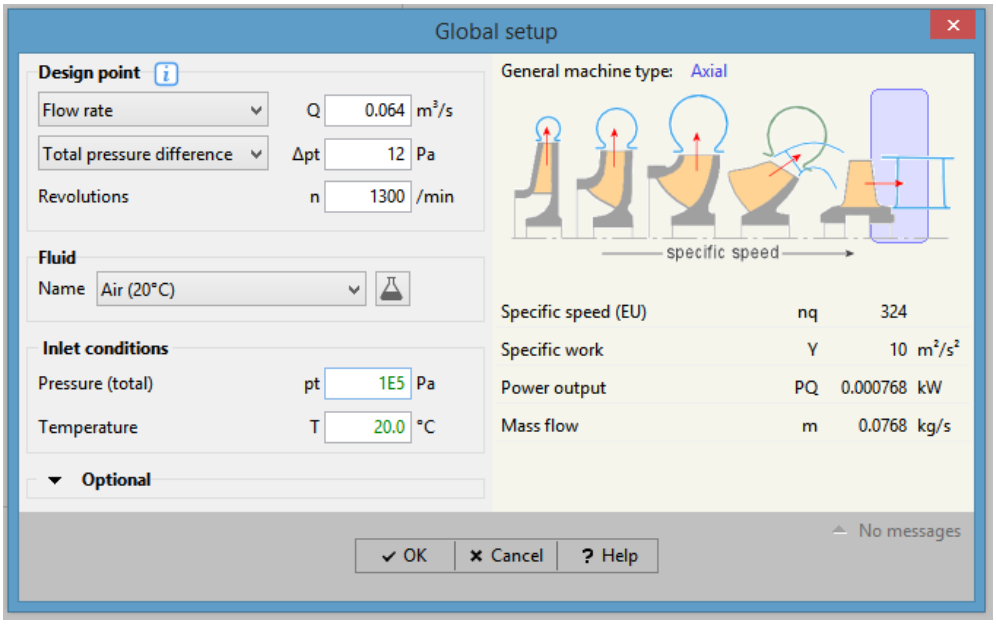

Figure 3.2: Design point values and machine type

3.3.2 Impeller Main Dimensions

The main dimensions menu item is used to define the main dimensions of the axial impeller. These main dimensions are considered as the most important basis for all the following design steps.

3.3.2.1 General setup

- The desired impeller is unshrouded. Thus, there is no need to set up the tip clearance value.
- The material density of the impeller is an informational value that is not relevant for the hydraulic design.
- The blade design mode is selected based on the blade average solidity value. Since the average blade solidity is less than 0.68, the airfoil approach is adopted

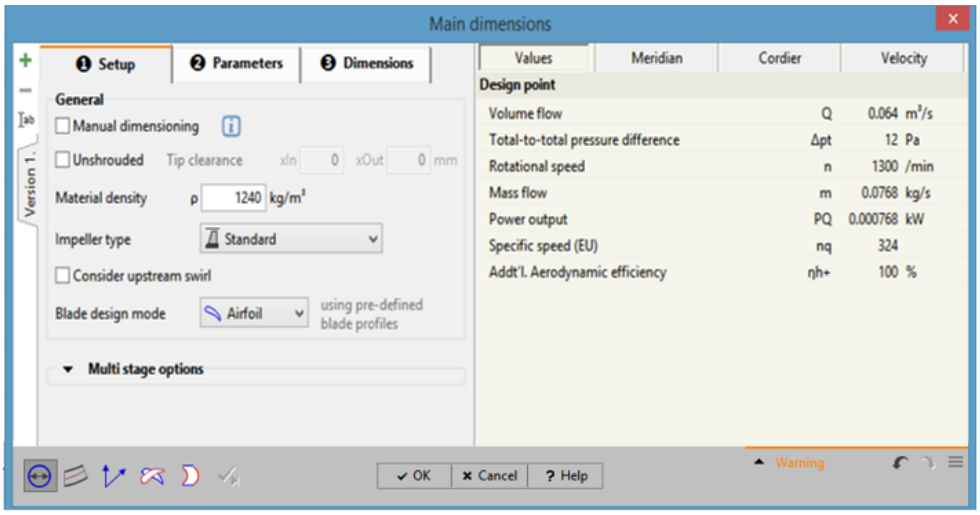

Figure 3.3: Impeller main dimensions (General setup)

3.3.2.2 Empirical parameters

This section illustrates the empirical parameters (flow coefficient and hub-tip ratio) resulting from approximation functions in reliance on the specific speed.

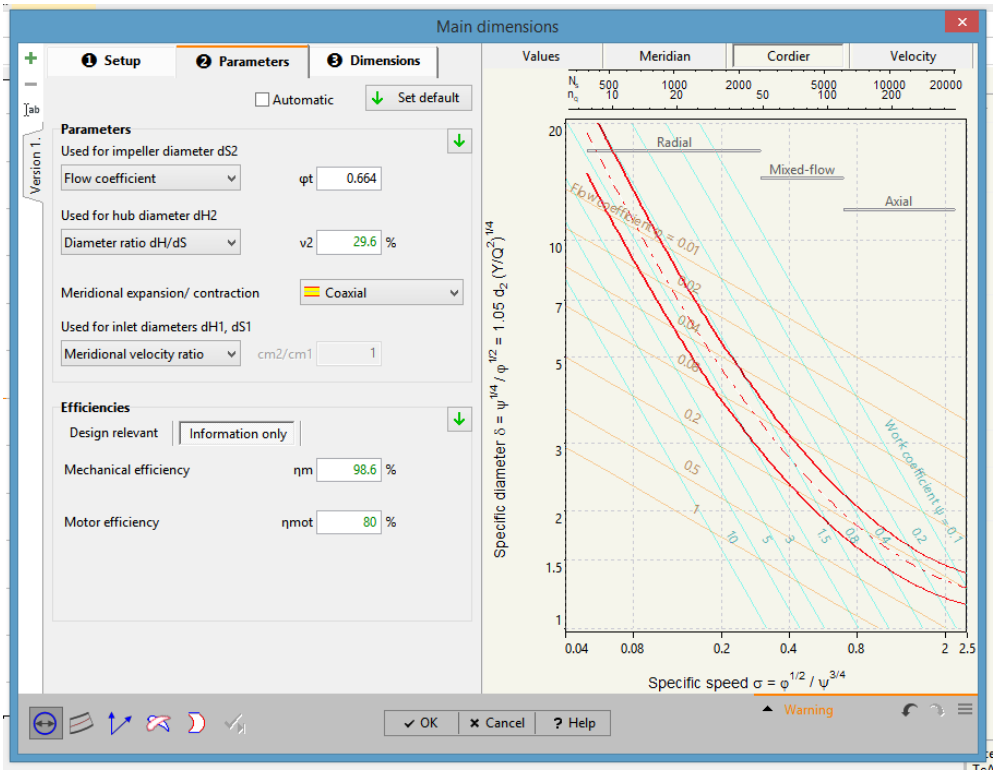

Figure 3.4: Impeller main dimensions (Empirical parameters)

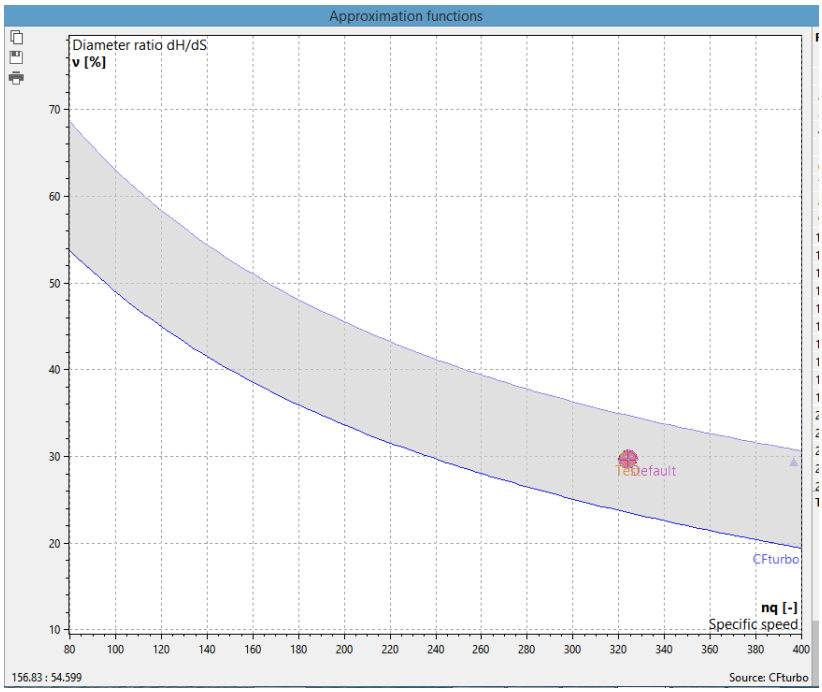

Figure 3.5: Approximation function (Hub-tip ratio)

After determining the hub-tip ratio, the hub diameter can be calculated as follows: $D_u = \vartheta D_t$ where $D_t = D_{fan} = 127$ mm the hub diameter as well as tip (shroud) diameter are illustrated in figure 6.3.

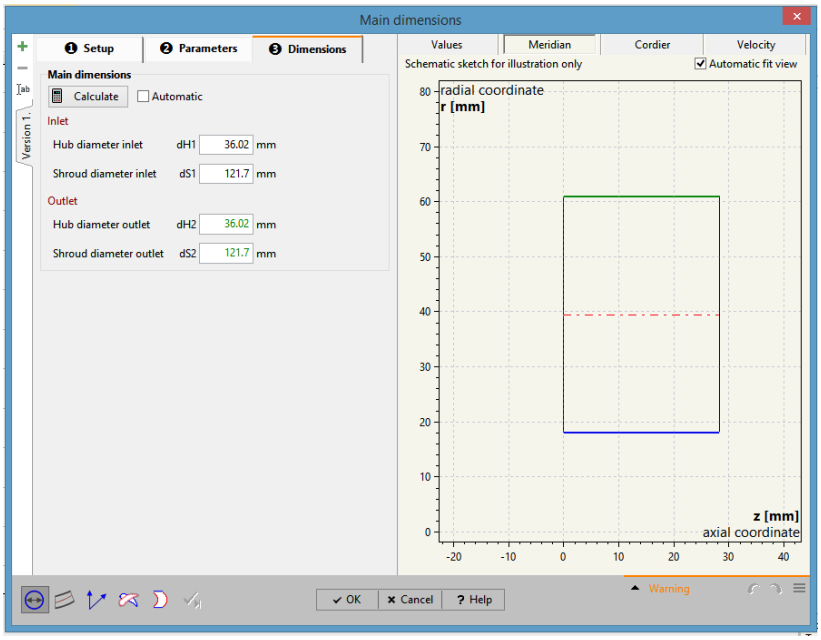

Figure 3.6: Values of hub and tip diameters

The computed variables resulting from calculated and determined main dimensions in accordance with the actual state of design are displayed in figure 7.3. Additionally, some adopted formulas for calculating these variables are given in table 2.3.

Table 3.2: the used formulas for calculating some variables

Work coefficient	$\psi = \frac{Y}{U_{2S}^2/2}$
Flow coefficient	$\varphi = \frac{Q}{\pi/4 d_{2S}^2 U_{2S}}$
Moeridional flow coefficient	$\varphi_m = \frac{Q_2}{\frac{\pi}{4}(d_{2S}^2 - d_{2H}^2)u_2} = \frac{c_{m2}}{u_2}$
Diamter coefficient	$\sigma = \frac{\psi^{1/4}}{\varphi_t^{1/2}} = 1.05 d_{2S} \left(\frac{Y}{Q_{ts}^2}\right)^{1/4}$
Average inlet velocity	$C_{m1} = \frac{Q}{\pi/4(d_{S1}^2 - d_{H1}^2)}$
Average outlet velocity	$C_{m2} = \frac{Q}{pi/4(d_{2S}^2 - d_{H2}^2)}$
outlet circ. Velocity component	$C_{u2} = \frac{1}{u_2}(Y - u_1 c_{u1})$

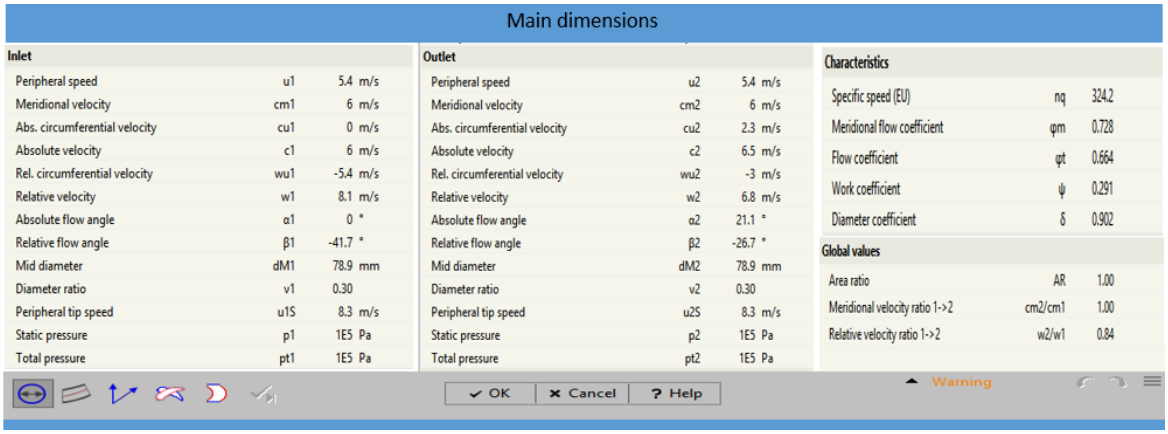

Figure 3.7: Results of mid-span calculation

The velocity triangles are the result of a mid-span calculation and they are based on the design point and the main dimensions. The velocity triangles at inlet and outlet are represented in figure 8.3.

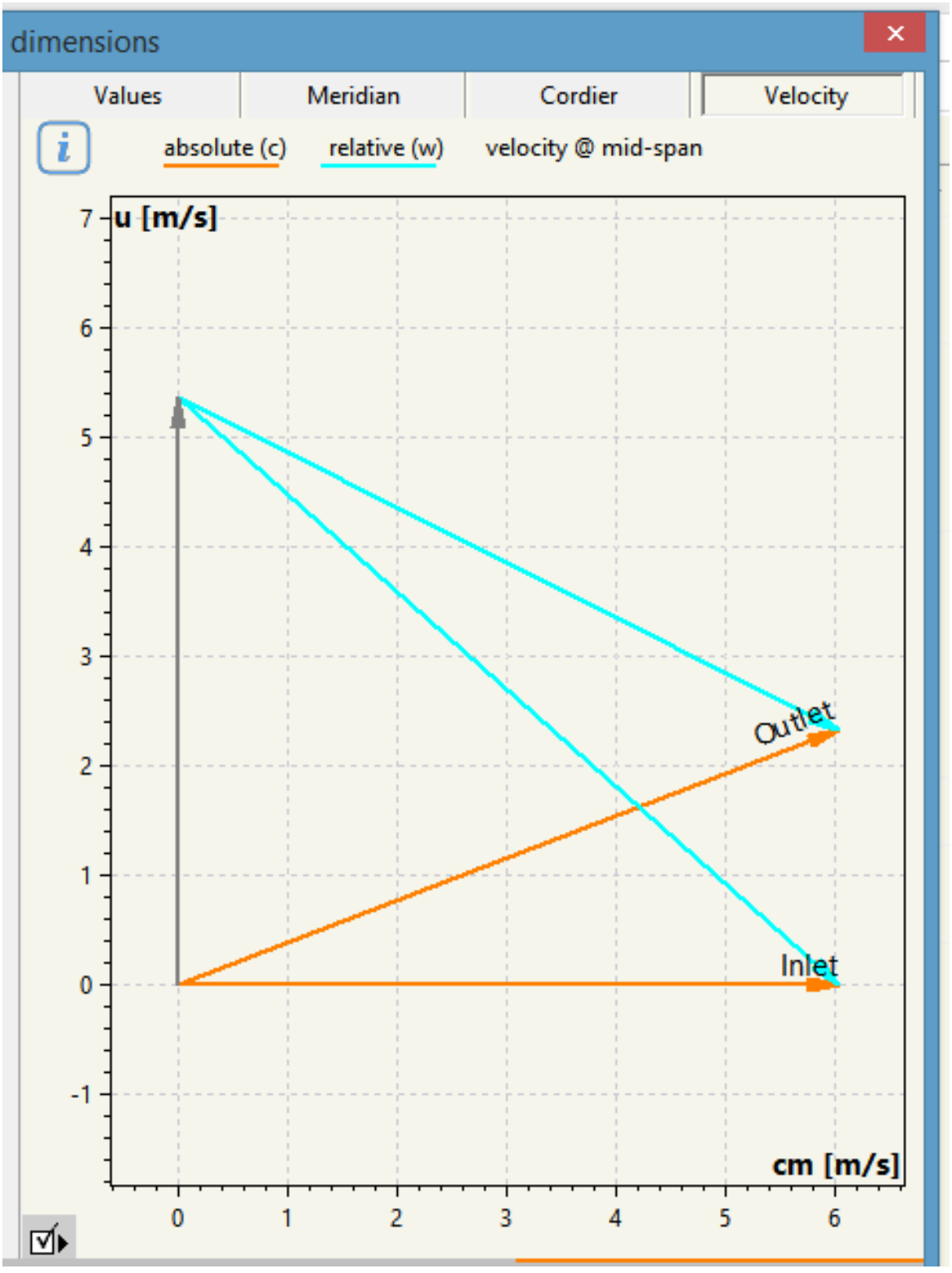

Figure 3.8: Velocity triangles

3.4 Impeller Meridional Contour

The meridional contour design is the second crucial phase in the impeller design process, it is divided into two main parts:

- Primary flow path
- Hub/Shroud solids

3.4.1 Primary Flow Path

This section contains the design of the primary flow path and it involves the definition of hub and shroud contours, as well as leading and trailing edge contour.

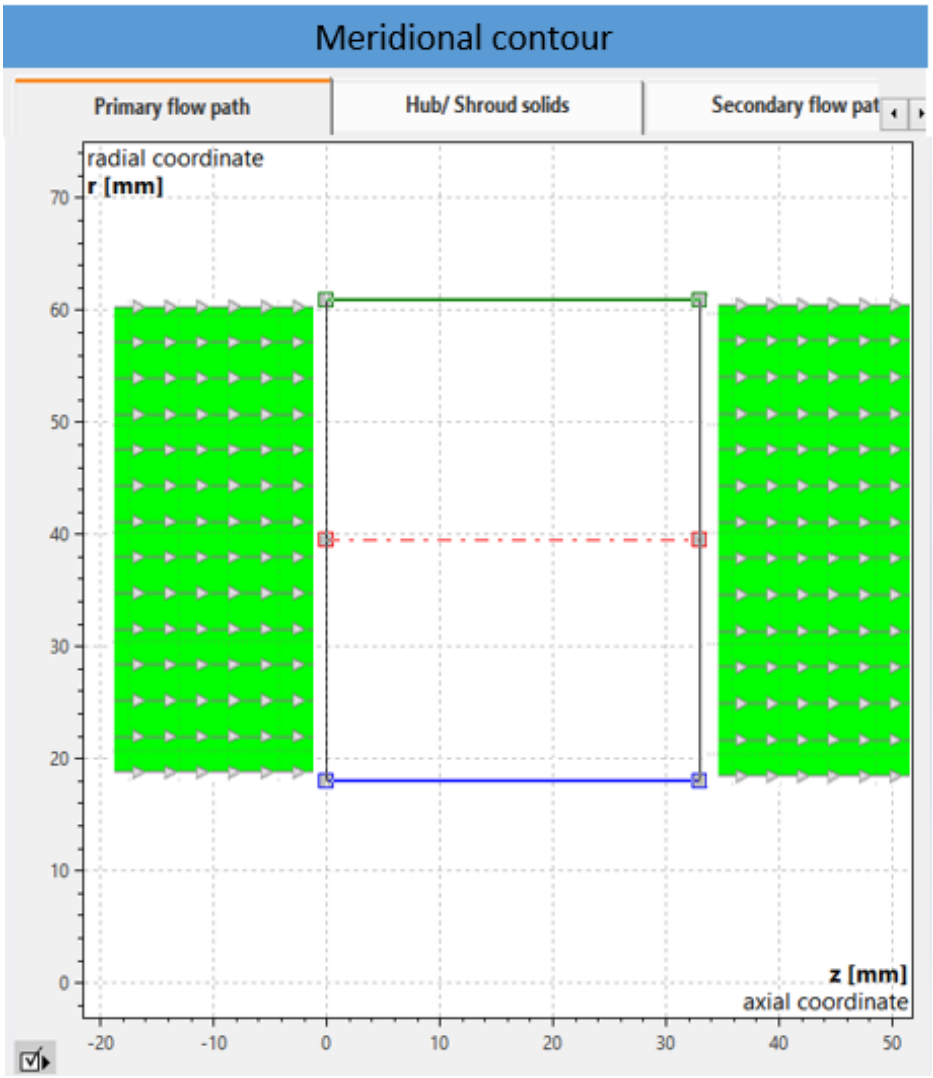

Figure 3.9: Primary flow path

3.4.2 Hub/Shroud solids

This phase contains the design of hub and/or shroud solids, it is an optional part that concerns stress analysis.

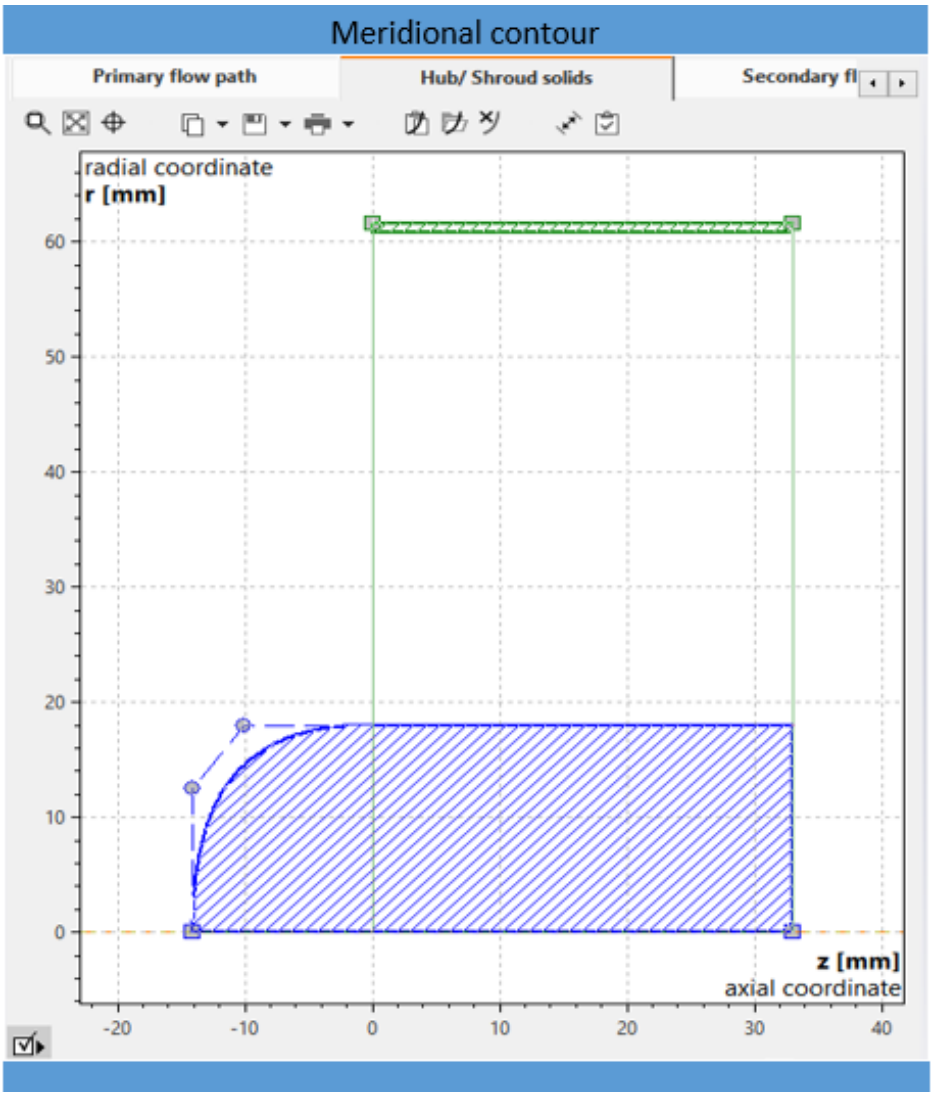

Figure 3.10: Hub solid

The global information values of the meridional contour design, and also the 3D hub model, are represented in table 4.3 and figure 11.3, respectively, after designing the primary flow path and specifying the hub and shroud contours, in addition to the hub solid.

Meridional contour

Informational values

Hub & Shroud				
		Hub	Shroud	
Angle on startpoint	ε1	0	0	°
Angle on endpoint	ε2	0	0	°
Axial extent	Δz	33	33	mm
Radial extent	Δr	0	0	mm
Axial extent blade	ΔzBl	33	33	mm
Radial extent blade	ΔrBl	0	0	mm
Inlet & Outlet				
Inlet angle		γIn	90	°
Outlet angle		γOut	90	°
Extents				
Axial extent max.		ΔzMax	33	mm
Radial extent max.		ΔrMax	42.84	mm
Diameter ratio		d1/d2	1.000	
Airfoil blade extent		ΔzMaxBl	29.94	mm

Figure 3.11: Meridional contour global information

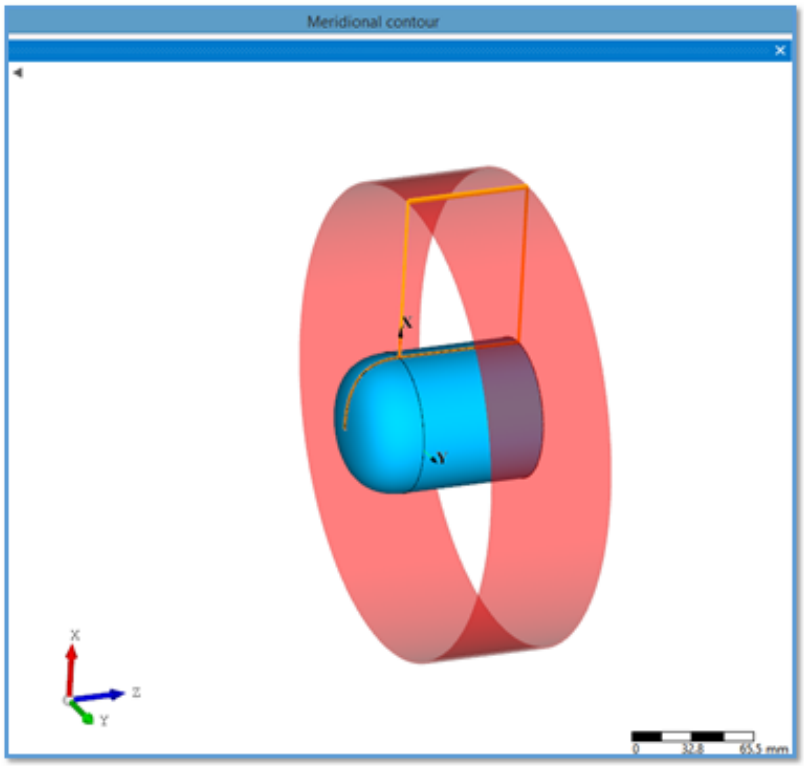

Figure 3.12: Hub 3D model

3.5 Blade's Geometry Design

The airfoil design approach is used to design the geometry of the blade based on the average solidity value, while the number of blades is determined by means of an approximation function based on the specific speed. It can be noted from the below graph that the number of blades corresponding to the specified speed is seven.

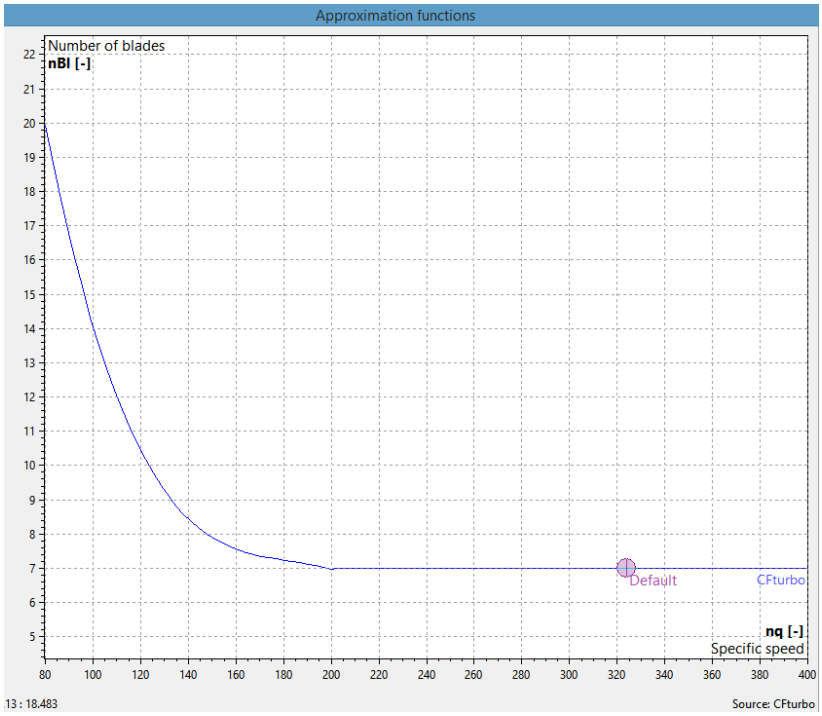

Figure 3.13: Number of blades in accordance to specific speed

According to the airfoil design mode, the geometry of the blade is generated in three steps:

- Blade properties
- Blade profiles
- Blade sweeping

3.5.1 Blade properties

There are three steps involved in defining blade properties:

- c_u , c_m specification

- Blade profile selection
- Stagger angle,chord length

3.5.1.1 specification

In this step, the radial equilibrium is used to define the c_u and c_m velocity distributions at each span. The free free vortex method is applied to determine the radial equilibrium from hub to shroud.

The velocity c_u and c_u distributions along the blade's radius, as well as the velocity triangles for the hub and shroud at the leading and trailing edges, are both shown in figure 13.3.Additionally, numerical values of velocity components and flow angles (at hub and shroud) are demonstrated in table 5.3.

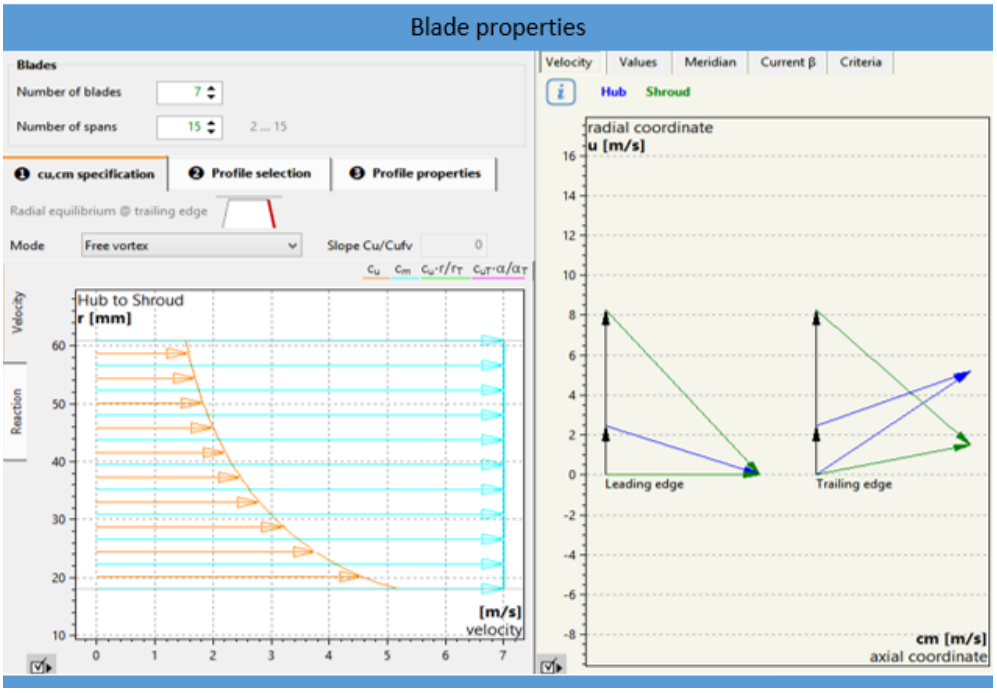

Figure 3.14: Number of blades in accordance to specific speed

Blade properties

	Span = 1 (Hub)		Span = 15 (Shroud)	
	Leading edge	Trailing edge	Leading edge	Trailing edge
z	0	33	0	33
d	36.02	36.02	121.7	121.7
αF	0	36.4	0	12.3
βF	-19.3	21.2	-49.8	-44
u	2.5	2.5	8.3	8.3
cm	7	7	7	7
cu	0	5.2	0	1.5
cr	0	0	0	0
cax	7	7	7	7
c	7	8.7	7	7.2
wu	-2.5	2.7	-8.3	-6.8
w	7.4	7.5	10.8	9.7
w2/w1	1.01		0.9	
c2/c1	1.24		1.02	
Δ(cu·r)	0.0931		0.0931	
T	0.00012		0.00039	
Δpt	15.21		15.21	

Figure 3.15: Numerical values of velocity components and flow angles at hub and shroud

Table 3.3: Nomenclture

z	Axial co ordinate
d	diameter
αF	angle of absolute flow to circumferential direction
βF	ange of relative flow to circumferential direction
u	circumferential velociy
c_m	Meridional veclocity
c_u	Circumferential compenent of absolute velocity
c_r	Radial component of absolute velocity
$c_a x$	axial component of absolute velocity
c	absolute velocity
w_u	circumferential component of relative velocity
w	relative velocity
w_2/w_1	deceleration ration of relative velocity
$\Delta\,(cu.r)$	Swirl difference
T	torque
Δp_t	Pressure difference

3.5.1.2 Blade profile selection

Cfturbo software provides a NACA profile catalog in the blade profile manager, from which the blade profile is specified. The blade profile selected for the present design is NACA6513.

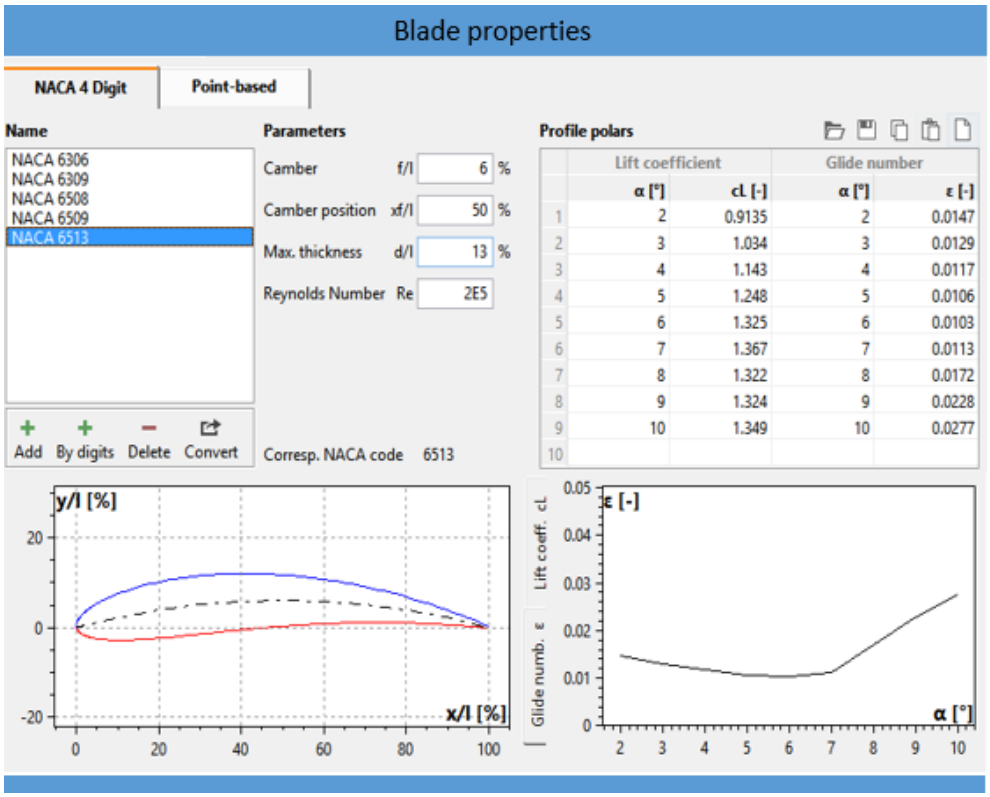

Figure 3.16: Number of blades in accordance to specific speed

The characteristics of the specified profile are depicted in table 6.3, where is the glide ratio is the angle of attack and the lift coefficient.

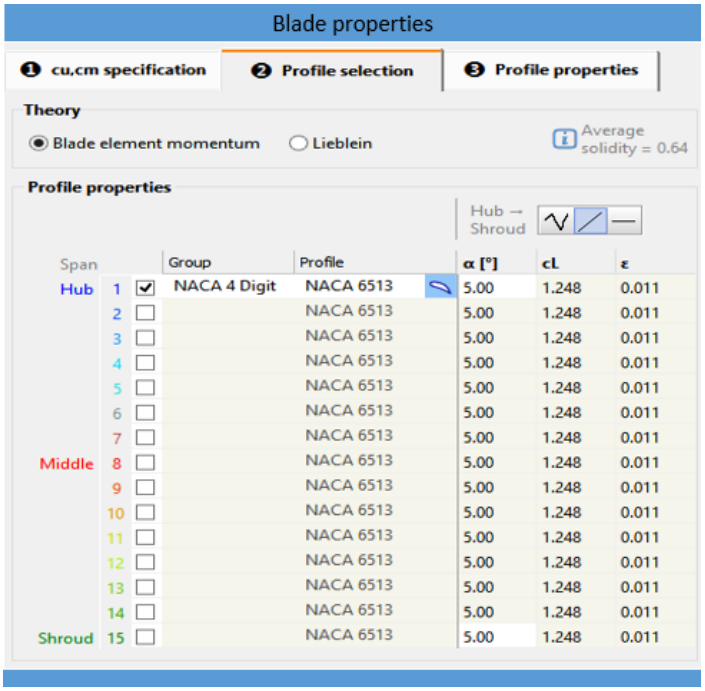

Figure 3.17: Properties of the blade profile

3.5.1.3 Stagger angle, chord length

The blade at each span is described by the stagger angle, chord length, and the specified profile. On the other hand, several diagrams with aerodynamic values and criteria are available to assess the blade profile, and if required profile parameters such as stagger angle and chord length can be adjusted.

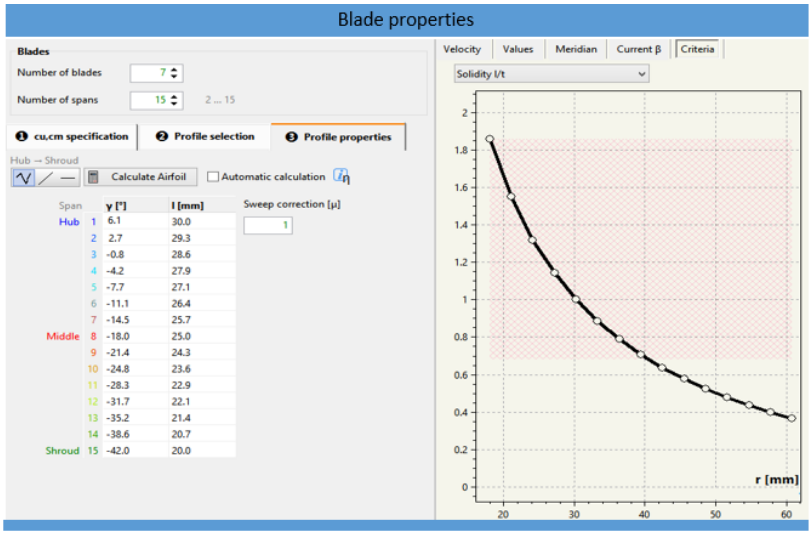

Figure 3.18: Blade stagger angle and chord length at different span

3.5.2 blade profile

In this phase 2D, also 3D blade profiles are created in accordance with the determined values from blade properties, where:

- The profile shape is based on the selected profile.
- The chord length and stagger angle of each profile at the respective span position are based on profile properties.

For NACA 4 digit, NACA 65 series profiles, the trailing edge thickness can be adapted for manufacturing reasons. The additional thickness is added linearly over the length of the profile.

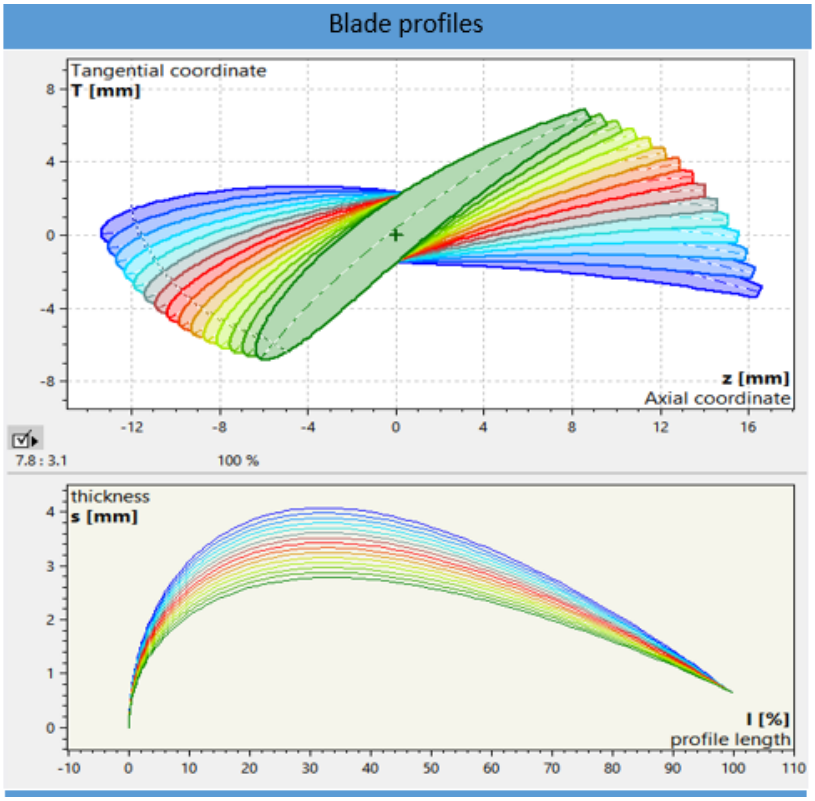

Figure 3.19: 2D profiles and thickness distribution at different span

The 3D blade profiles are shown in figure 17.3.

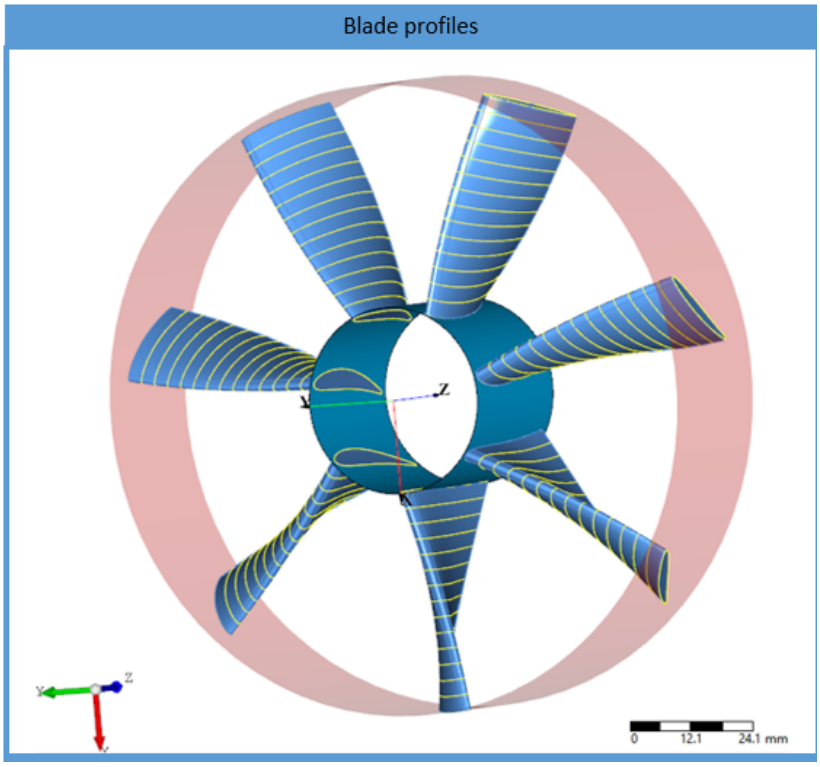

Figure 3.20: 3D blade profiles

3.5.3 Blade sweeping

In this design stage, the blade sweep can be optionally specified. Blade sweep is normally useful for acoustic reasons and comes at the cost of slightly reduced efficiency. This design step was not included in the present design, it is only referred to.

At the end of this step, the 3D fan geometry is finally generated and after making the necessary revisions it can be exported for CFD simulation.

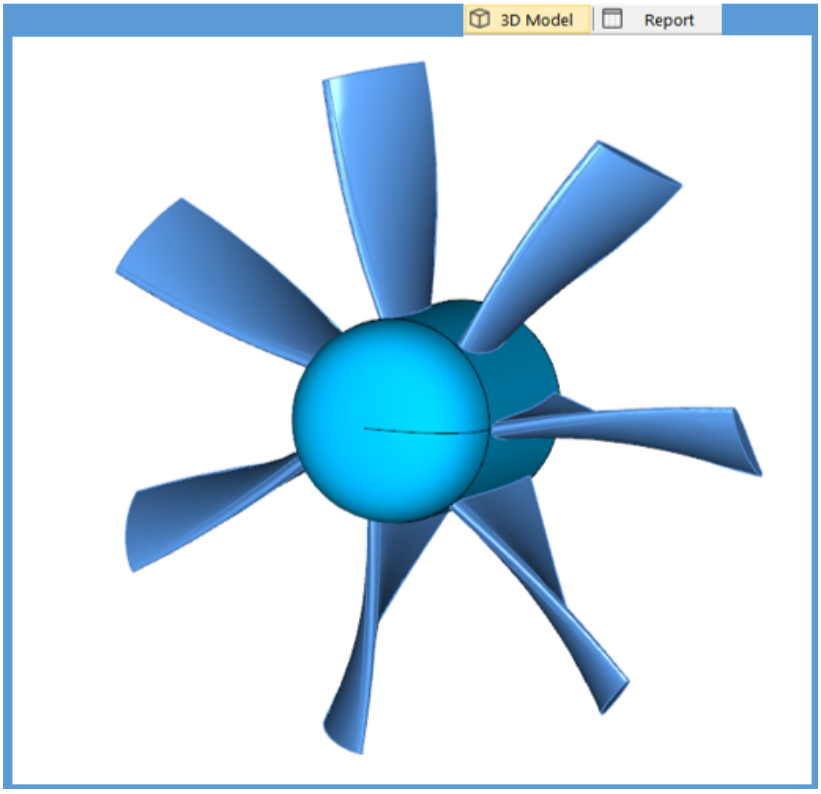

Figure 3.21: 3D axial flow fan model

Chapter 4

CFD Analysis of the Axial Flow Fan

4.1 Introduction

The information about the fluid flow characteristics and flow parameters such as pressure, velocity, and temperature, as well as the aerodynamic properties in the designed model, can be investigated using Computational Fluid Dynamics (CFD) techniques, which require the resolution of the basic fluid dynamics equations, such as mass and momentum conservation equations for pressure and velocity, and the energy equation for the temperature. The solution of these undefined variables demands the use of a specific procedure, which is where CFD comes in.Computational fluid dynamics (CFD) is a technique for numerically solving a set of differential equations that characterize fluid flow and related phenomena to obtain specific information about the flow field. Despite the fact that this efficient technique is constantly evolving and new approaches are being developed, satisfactory results for engineering issues are being achieved. Interestingly, when experimental testing is not practicable, The computational fluid dynamics (CFD) technique is often employed. Furthermore, it is considered as a refinement tool for the proposed model, allowing the prevention or minimization of design mistakes before passing to the manufacturing process [10] .

In this work, The CFD analyses of the axial flow fan are carried out using a commercial CFD software, Ansys-Fluent. Where the 3D designed geometry is exported from CFturbo to Gambit 2.0 software, which generates the mesh model. The study is then launched after the boundary conditions and turbulence model have been set up.

4.2 Geometry

Since the phenomenon of flow passing across the fan from inlet to outlet occurs in a periodic way, the analytic study is only carried out in a single fan blade then the obtained information is generalized to the rest of the blades. Figure 4.1 illustrates a single 3D blade shape of the axial flow fan inside the flow domain, it can be seen that the blade has a twisted shape due to increasing stagger angle from the hub to the tip.

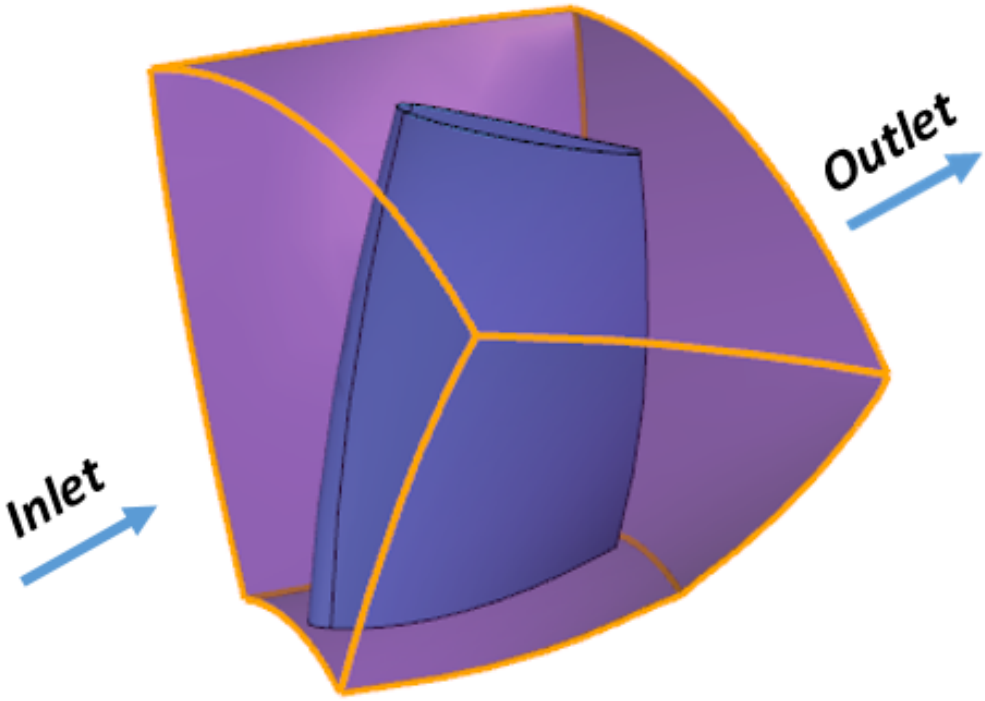

Figure 4.1: The Axial fan single 3D blade shape inside the flow domain

4.3 Computation Mesh

The meshing section of the analysis is critical to obtaining correct fluid flow at the end of the numerical calculations. As a result, the type, size, number of elements and nodes, and other geometric aspects of the mesh should be defined in accordance to the geometric properties of the axial flow fan.

The computational mesh of the solution domain consists of both tetrahedral quadrilateral and elements. As it mentioned earlier, since the flow domain is repeated in every blade, so that the entire domain is not modeled for the required solution, only

the volume around one blade is meshed. The number of cell elements in the domain is approximately 82830 and number of nodes is 17669. Figure 2.4 shows the computational mesh of the solution. In the figure, the shroud elements are not shown to make the blade visible.

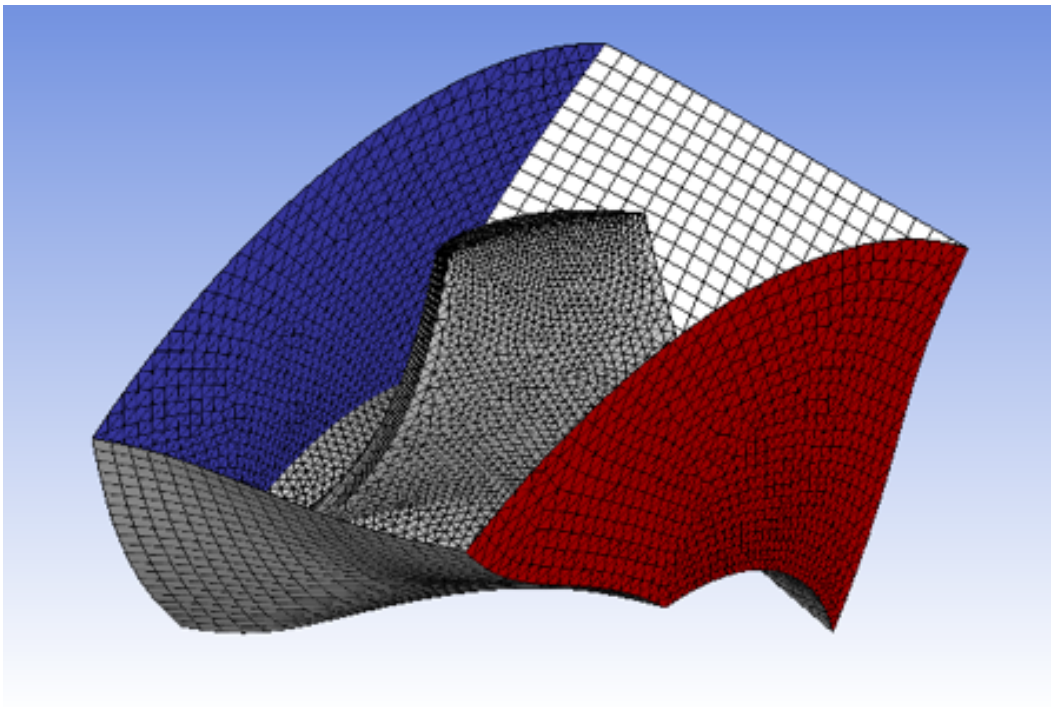

Figure 4.2: Computational mesh of the solution domain

4.4 Boundary Conditions

The operating conditions are processed by the analytical software via boundary conditions. The mesh's inlet and outlet faces are flow inlet and outlet type boundaries, respectively, whereas the mesh's side faces are periodic boundaries. Besides, the velocity inlet boundary and the pressure outlet boundary are specified on the inlet and outlet faces, respectively. The periodic boundary conditions are set rotationally periodic. The boundary conditions of the solution domain are illustrated in figure 3.4 and figure 4.4.

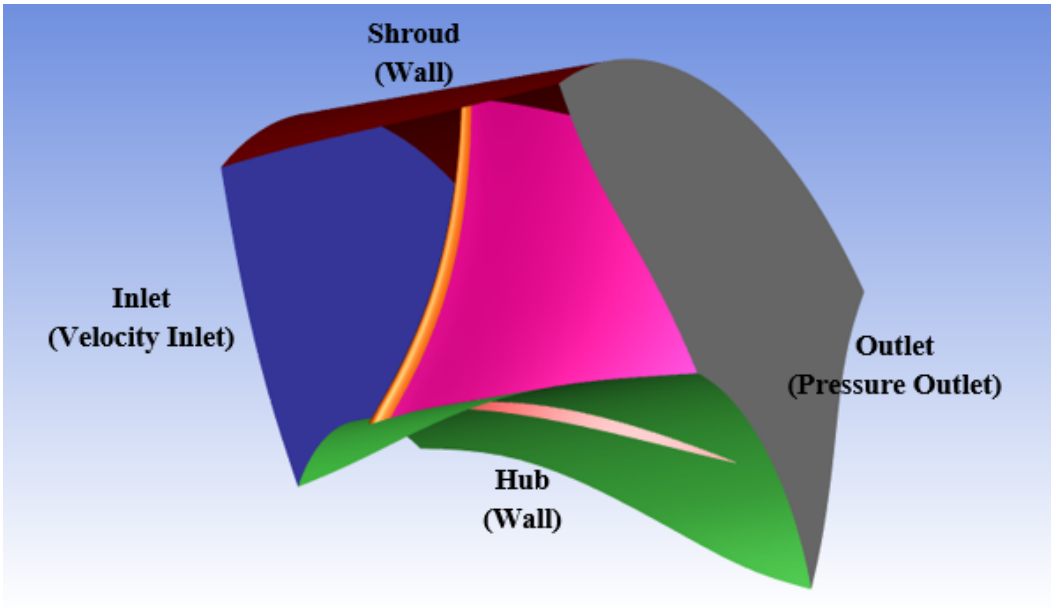

Figure 4.3: Fan Boundary Conditions (1)

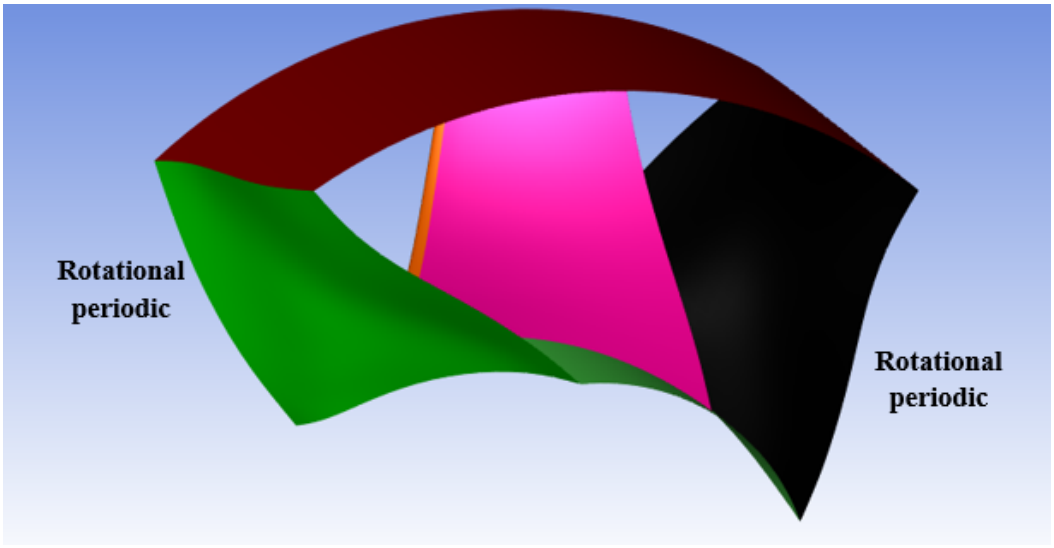

Figure 4.4: Fan Boundary Conditions (2)

4.5 Turbulence Model and Solver Options

General Conclusion

This work has enabled us to design a 3D model of an axial flow fan using modern, sophisticated software as well as realize the fan model by means of a 3D printer, thus enhancing and enriching our knowledge in the field of turbomachinery and, more specifically, in the axial flow fans domain.It is noted during this work that the design process of an axial flow fan is complicated and lasts long and also requires a thorough understanding of a variety of areas such as fluid mechanics, turbomachinery and last but not least aerodynamics.Additionally, the design procedure is remarkably based on empirical graphs and functions and also includes different design approaches.

Bibliography

[1] H. Ö. Kekliko, "Design, construction and performance evaluation of axial flow fans," 2019.

[2] T. Köktürk, "Design and performance analysis of a reversible axial flow fan," Master's thesis, 2005.

[3] S. M. Yahya, *Turbines compressors and fans*. Tata McGraw-Hill Education, 2010.

[4] F. P. Bleier, *Fan handbook: selection, application, and design*. McGraw-Hill, 2018.

[5] S. Castegnaro, "Fan Blade Design Methods: Cascade Versus Isolated Airfoil Approach—Experimental and Numerical Comparison," in *Turbo Expo: Power for Land, Sea, and Air*, vol. 49682, p. V001T09A007, American Society of Mechanical Engineers, 2016.

[6] P. Epple, F. Durst, and A. Delgado, "A theoretical derivation of the Cordier diagram for turbomachines," *Proceedings of the Institution of Mechanical Engineers, Part C: Journal of Mechanical Engineering Science*, vol. 225, no. 2, pp. 354–368, 2011.

[7] G. T. Csanady, "Theory of turbomachines," tech. rep., McGraw-Hill, 1964.

[8] S. L. Dixon and C. Hall, *Fluid mechanics and thermodynamics of turbomachinery*. Butterworth-Heinemann, 2013.

[9] X. Dachuan, W. Haifeng, Q. Xiaoli, Y. Yongsheng, S. Yu, and Z. Fang, "Application of Arbitrary Vortex Method in Wind Tunnel Axial Fan Design," in *IOP Conference Series: Materials Science and Engineering*, vol. 616, p. 12006, IOP Publishing, 2019.

[10] A. C. Yunus, *Fluid Mechanics: Fundamentals And Applications (Si Units)*. Tata McGraw Hill Education Private Limited, 2010.